Surface modification of a Mo-substrate to form an oxidation-resistant MoSi$_2$ layer using a Si-saturated tin bath

Jonah Gamutan [*], Takahiro Miki

Department of Metallurgy, Graduate School of Engineering, Tohoku University, Aobayama 6-6-02, Sendai 980-8579, Japan

ARTICLE INFO

ABSTRACT

Molybdenum disilicide (MoSi$_2$) is one of the most heat and oxidation resistant materials used in high-temperature applications. In this work, the feasibility of forming an oxidation-resistant MoSi$_2$ coating using a low-temperature Sn-Si bath by the hot dipping method was evaluated. It was found that a smooth and dense MoSi$_2$ layer can be successfully synthesized on the surface of a Mo-substrate at 700 °C to 1000 °C. Using this method, MoSi$_2$ can be synthesized more rapidly than using conventional methods and at much low operating temperatures. The diffusion through the product layer controlled the growth of the formed MoSi$_2$ layer, and the growth rate was fastest at 800 °C. This was due to the replacement by the larger tin atoms that led to the expansion of the lattice, allowing the faster diffusion of silicon through the silicide layer towards the unreacted Mo-substrate. Oxidation resistance test at 1150 °C for 2 h confirmed that the MoSi$_2$ layer formed by the present method protects the Mo-substrate from rapid oxidation at elevated temperatures.

1. Introduction

Due to their excellent heat and oxidation resistance, molybdenum disilicide (MoSi$_2$) and MoSi$_2$-based composites are widely used in high-temperature applications, even under oxidizing environments [1,2]. However, the use of MoSi$_2$ is limited by the constraints of compression manufacturing, which makes the production of large components and complex shapes impossible. Meanwhile, refractory metals such as molybdenum and its alloys are considered highly attractive materials for use in high-strength high-temperature applications due to their high melting points (2623 °C), excellent electrical and thermal conductivities, and low coefficient of thermal expansion (5.5 × 10^{-6} °C^{-1}) [3]. Molybdenum superalloys, such as the Mo-Si-B-based alloys, are considered the next-generation materials to replace nickel super alloys in the heat engines in power plants, propulsion systems in aerospace applications, and high-temperature electrodes in metallurgical processes [4]. However, the poor oxidation resistance of molybdenum in high-temperature environments is a serious limitation, restricting its widespread use. Under oxidizing conditions, molybdenum readily reacts with oxygen to form highly volatile molybdenum oxide species, such as MoO$_3$ and MoO$_2$, which degrades the material and eventually leads to its failure [5].

To improve the high-temperature oxidation resistance of molybdenum and its alloys, modification of the surface to provide an oxidation-resistant layer that prevents direct contact between oxygen in the atmosphere and the substrate is necessary. At present, formation of a silicide layer on the surface of molybdenum has been found to provide the best protection at high temperatures. MoSi$_2$ has both a high melting point (2030 °C) and the ability to form a self-healing protective SiO$_2$ layer at the material surface that can prevent the Mo-substrate from further oxidation. It also has a comparably high thermal conductivity, which is beneficial for increased cooling efficiency of a component, and a low coefficient of thermal expansion (8.1 × 10^{-6} °C^{-1}) that roughly matches that of the Mo-substrate, imparting lower thermal stresses and minimizing interfacial crack formation [1]. Over-all, surface modification of a Mo-substrate to form MoSi$_2$ has a huge potential to improve the already impressive heat resistance of molybdenum and its alloys.

Several techniques have already been developed to produce MoSi$_2$ parts and coatings. These techniques, which are summarized in Table 1, include halide-activated pack cementation (HAPC) [6–9], slurry sintering [10–12], spark plasma sintering (SPS) [13–16], chemical vapor deposition [17–20], and the hot dipping method [21–28]. Among these, pack cementation is the most common method of siliconizing the surface of a Mo-substrate. However, this method is associated with significant problems, including a lengthy preparation time and difficulty controlling the coating thickness. Its use is also restricted to small parts and

uncomplicated shapes. In the case of slurry sintering and spark plasma sintering, the porosities of the obtained coating are both high, significantly limiting the oxidation resistance at high temperatures. The equipment used in the chemical vapor deposition method is prone to damage and corrosion due to high-temperatures and severe process conditions. The short treatment time, and the simple and straightforward procedure of the hot dipping method, combined with its ability to modify the surface of large and complex components, suggests it is the most effective $MoSi_2$ surface modification technique.

Several research groups have successfully siliconized molybdenum and its alloys using various Si-containing molten alloy baths. For example, Zhang et al. used a pure molten Si bath to synthesize a Si-$MoSi_2$ layer at the surface of a Mo-based alloy at 1480 °C to 1560 °C. Their results showed the formation of a multi-layer structure consisting of Si, $MoSi_2$, Mo_5Si_3, and Mo_3Si layers [21–24]. In another study, Christian et al. used an In-Si dipping alloy in a sealed quartz ampoule under vacuum conditions at 1000–1200 °C. Their results showed the formation of a $MoSi_2$ layer and a thin Mo_5Si_3 interlayer [25]. In other studies, an Al-Si melt was used as the dipping alloy, which led to the formation of a $Mo(Si,Al)_2$ layer at temperatures between 700 °C and 1000 °C [26–28].

However, using silicon and aluminum-based molten baths is expensive and requires dipping temperatures above the melting points of silicon (1410 °C) and aluminum (660 °C). In addition, hot dipping using the In-Si molten bath demands the use of indium, which is a rare and highly volatile element. Therefore, there is a demand for a silicon bath made from readily available materials, is inexpensive, and with a low-melting temperature. Tin (Sn) is an excellent candidate as a hot dipping alloy due to its low melting temperature (232 °C), availability, and cost. In addition, according to the Sn-Si and Sn-Mo binary phase diagrams [29,30], the solubility of tin into silicon and molybdenum is almost negligible, which means that when molybdenum is dipped into the Sn-Si melt, molybdenum reacts only with silicon, forming $MoSi_2$. However, the feasibility of this process, the rate at which $MoSi_2$ forms and the oxidation resistance of the formed $MoSi_2$ layer using the proposed method remain unknown. Therefore, in this study, the feasibility of using a Si-saturated molten tin bath to modify the surface of a Mo-substrate to form an oxidation-resistant $MoSi_2$ layer was investigated. Specifically, the phase composition of the layers, their growth characteristics, and the oxidation resistance of the modified surfaces were determined.

2. Experimental method

Commercially available molybdenum sheet (99.95 % purity, NILACO Co.) cut into $1 \times 10 \times 50$ mm plates were used as the substrate in the experiments. The samples were polished using SiC paper with up to a 1000 mesh and then ultrasonically cleaned in ethanol for 10 min. The surface of the Mo-substrate was modified to $MoSi_2$ by immersing into the molten Sn-Si alloy employing a molybdenum wire (φ 2 mm). The siliconizing process was carried out at temperatures of 700 °C, 800 °C, 900 °C, and 1000 °C for 15, 30, and 60 min in an Ar gas atmosphere (400 ml min^{-1}).

The dipping alloy was prepared from reagent-grade tin shots and silicon lumps at the target composition of 98.8Sn-1.2Si (mass%). Under the temperature conditions used in this study, this alloy composition exists within the two-phase region of the Sn-Si phase diagram [29], consisting of a liquid Sn-Si phase and solid silicon. Due to the negligible solubility of tin into silicon, the thermodynamic activity of silicon can be assumed to be close to unity, such that $MoSi_2$ is expected to form on the surface of the Mo-substrate. Therefore, varying silicon concentration in the bath is not expected to influence coating structure and growth, unless the concentration is within the liquid only region of the Sn-Si phase diagram. In such case, the thermodynamic activity of Si falls below unity, and $MoSi_2$ may or may not form on the surface of the Mo-substrate.

After siliconizing, the Mo-substrates were taken out of the molten bath towards the cold zone within the top part of the furnace and then allowed to cool to room temperature. Any excess melt that adhered to the surface of the samples was dissolved in concentrated nitric acid (HNO_3) solution and removed by ultrasonic cleaning in ethanol.

To investigate the oxidation resistance of the siliconized samples using the Sn-Si melt, an isothermal oxidation test was carried out in a muffle furnace at 1150 °C for 2 h in air. The samples were initially placed in the furnace at room temperature and then heated up to 1150 °C for 1 h. After holding the temperature at 1150 °C for another 2 h, the power to the furnace was cut off and the samples were allowed to cool down inside the furnace. For comparison, tests were conducted for both bare and siliconized samples. Before the test, the edges of the samples were protected using a SiO_2 ceramic paste. To determine the extent of the oxidation reactions, changes in the weight of the sample before and after testing were monitored. The phase composition of the layers was characterized using X-ray diffraction (Ultima IV, Rigaku) from 10° to 90° with Cu-Kα radiation at a 5° min^{-1} scanning speed. The data were then analyzed and indexed using Rigaku PDXL software. The morphology and composition of the sample cross-section were analyzed using a Scanning Electron Microscope (SEM, JEOL JSM-6510) equipped with an Energy Dispersive Spectrometer (EDS, Oxford INCA Energy 250XT).

Table 1

Operating parameters and growth of $MoSi_2$ layer using a Mo-substrate using existing siliconizing techniques [6–12,14,17–28].

Method	Material used	Temperature (°C)	Growth rate (μm/h)	Ref.
Halide-activated pack cementation (HAPC)	10Si–10NH$_4$F–80(Al$_2$O$_3$/SiO$_2$/SiC)	1300	9.0	[6]
	10Si–10NH$_4$F–80Al$_2$O$_3$	1100	4.7	[7]
	25Si–5NaF–70Al$_2$O$_3$	900	0.3	[8]
	55Si–1NaF–44Al$_2$O$_3$	900	1.5	[9]
Slurry sintering	Si–10Mo–15Ti	1450	480	[10]
	30Mo–69.5Si–0.5PVB	900	100	[11]
	36.85NaCl–36.58KCl–21.95NaF–4.89Na$_2$SiF$_6$	900	6.7	[12]
Spark plasma sintering (SPS)	MoSi$_2$–MoB–ZrO$_2$	1500	300	[14]
Chemical vapor deposition (CVD)	SiCl$_4$–H$_2$ gas	1200	6.0	[17]
	Si target	1000	10.0	[18]
	SiCl$_4$–H$_2$ gas	1150	166.7	[19]
	90Si–10Al	1100	85.0	[20]
Hot dipping method	Si bath	1480–1560	120	[21–24]
	In–Si bath	1000, 1200	2.8, 7.2	[25]
	Al–12%Si bath	950	33.3	[26]
	Al–26%Si bath	700	0.9	[27]
	Al–50%Si bath	1000	35.0	[28]

3. Results and discussion

3.1. Phase composition and growth

The x-ray diffraction patterns of the bulk Mo-substrate samples after siliconizing in a molten Sn-Si bath for 15 min at 700 °C, 800 °C, 900 °C, and 1000 °C are shown in Fig. 1. At 800 °C, 900 °C, and 1000 °C, the formation of $MoSi_2$ with a strong preferred orientation on the (103) crystal face was observed. Presence of other silicide compounds of molybdenum, such as Mo_5Si_3 and Mo_3Si, was not observed at these dipping temperatures, indicating that the phase composition of the formed coating does not change with temperature. These results also indicate that the formation of $MoSi_2$ at the surface of the Mo-substrate occurred as expected, considering that the thermodynamic activity of silicon in this melt was close to unity. Meanwhile, peaks of $MoSi_2$ were not observed after dipping the Mo-substrate at 700 °C for 15 min.

The influence of dipping time on the phase composition of the formed $MoSi_2$ layer at 1000 °C is shown in Fig. 2. While the peaks of the Mo-substrate were still strongly observed after dipping for 15 min, their intensity relative to the peaks of $MoSi_2$ decreased gradually with dipping time. The characteristic peaks of tin were also present in the x-ray diffraction data, indicating that the residual melt was not completely removed from the surface even after the cleaning step. The formation of other silicide compounds of molybdenum, was not observed even with increasing dipping time, suggesting that the phase composition of the formed coating does not change with time.

An SEM micrograph and EDS mapping of the sample cross-section are shown in Fig. 3, and the results of the area analysis are shown in Table 2. Area analysis results show that Mo:Si atomic ratio of the formed layer was approximately 1:2, confirming that the main phase composition is $MoSi_2$. It was also found that the formation of a dense $MoSi_2$ layer and a relatively smooth surface was successfully achieved. Although XRD analysis did not indicate the formation of $MoSi_2$ at 700 °C, SEM-EDS analysis confirmed the formation of a thin 4 μm $MoSi_2$ layer. The
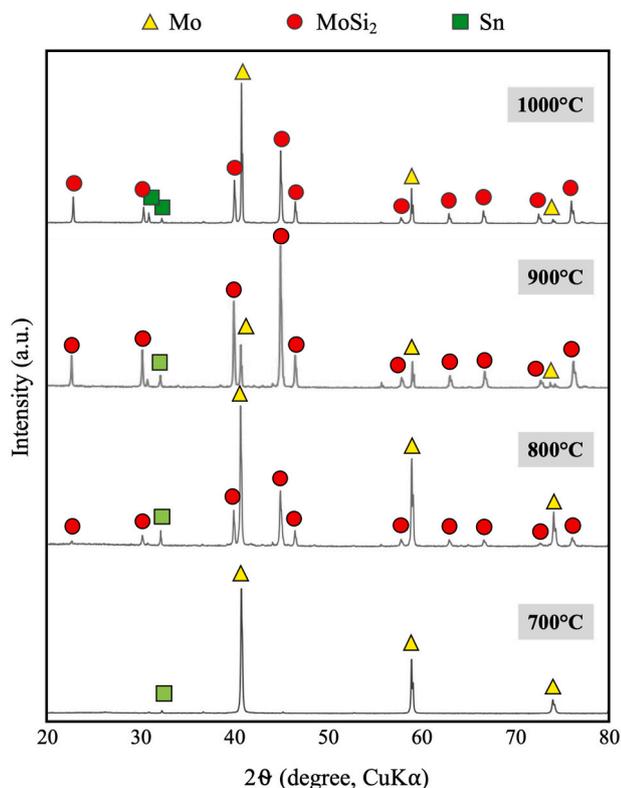
Fig. 1. XRD patterns of the molybdenum samples after hot dipping in a silicon-saturated tin bath for 15 min at 700 °C, 800 °C, 900 °C, and 1000 °C.
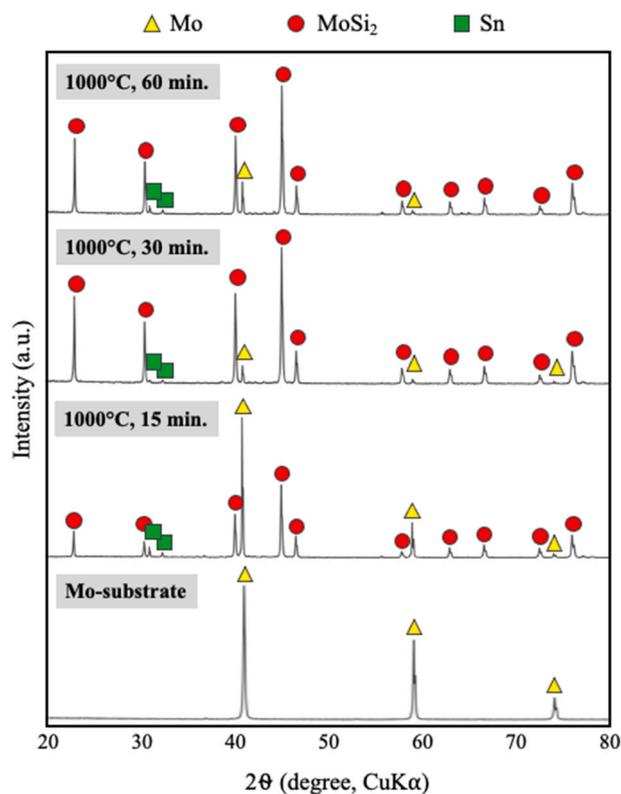
Fig. 2. XRD patterns of the molybdenum samples before and after hot dipping at 1000 °C for 15, 30, and 60 min.

presence of other silicide compounds of molybdenum was not observed as well.

After dipping for 15 min, the thickness of the formed $MoSi_2$ layer varied with temperature, as follows: 800 °C (28 μm) > 900 °C (13 μm) > 1000 °C (10 μm) > 700 °C (4 μm). An area analysis of the formed $MoSi_2$ layer after dipping at 800 °C and 900 °C showed the presence of approximately 6.43 and 4.68 mass% Sn in the $MoSi_2$ layer, respectively. Meanwhile, tin concentrations in the $MoSi_2$ layer were relatively low after dipping at 700 °C and 1000 °C. These results suggest that at intermediate dipping temperatures, the presence of tin in the $MoSi_2$ layer facilitated the diffusion of silicon, leading to the faster procession of the surface modification. In other words, the rapid growth of the $MoSi_2$ layer at 800 °C was made possible due to the presence of tin that introduced defects in the $MoSi_2$ crystals that allowed the faster diffusion of silicon through the silicide layer towards the unreacted Mo-substrate.

Cross-section micrographs of the formed $MoSi_2$ layer on the Mo-substrate after hot dipping at 800 °C for 15, 30, and 60 min are shown in Fig. 4. It was found that the depth of the formed $MoSi_2$ layer increased with dipping time and that a 43.4 μm thick coating forms after dipping for 60 min. These results indicate that even at a relatively low dipping temperature of 800 °C, the growth of the $MoSi_2$ layer proceeded at five times the speed reported for the conventional pack cementation method, which is carried out at 1300 °C [6].

The logarithms of the $MoSi_2$ growth rates as a function of temperature using various siliconizing techniques are shown in Fig. 5 for comparison purposes. Although $MoSi_2$ growth rates are one order of magnitude greater when using slurry sintering, spark plasma sintering, and chemical vapor deposition, the extremely high operating temperatures (1000 °C to 1500 °C), harsh treatment conditions, and increased coating porosity associated with these methods make them impractical for commercial use. Compared to the other hot dipping methods and the more commonly used pack cementation technique, the Sn-Si bath technique used in this study offers the fastest $MoSi_2$ growth rates even at low operating temperatures. In addition, it was found that the $MoSi_2$
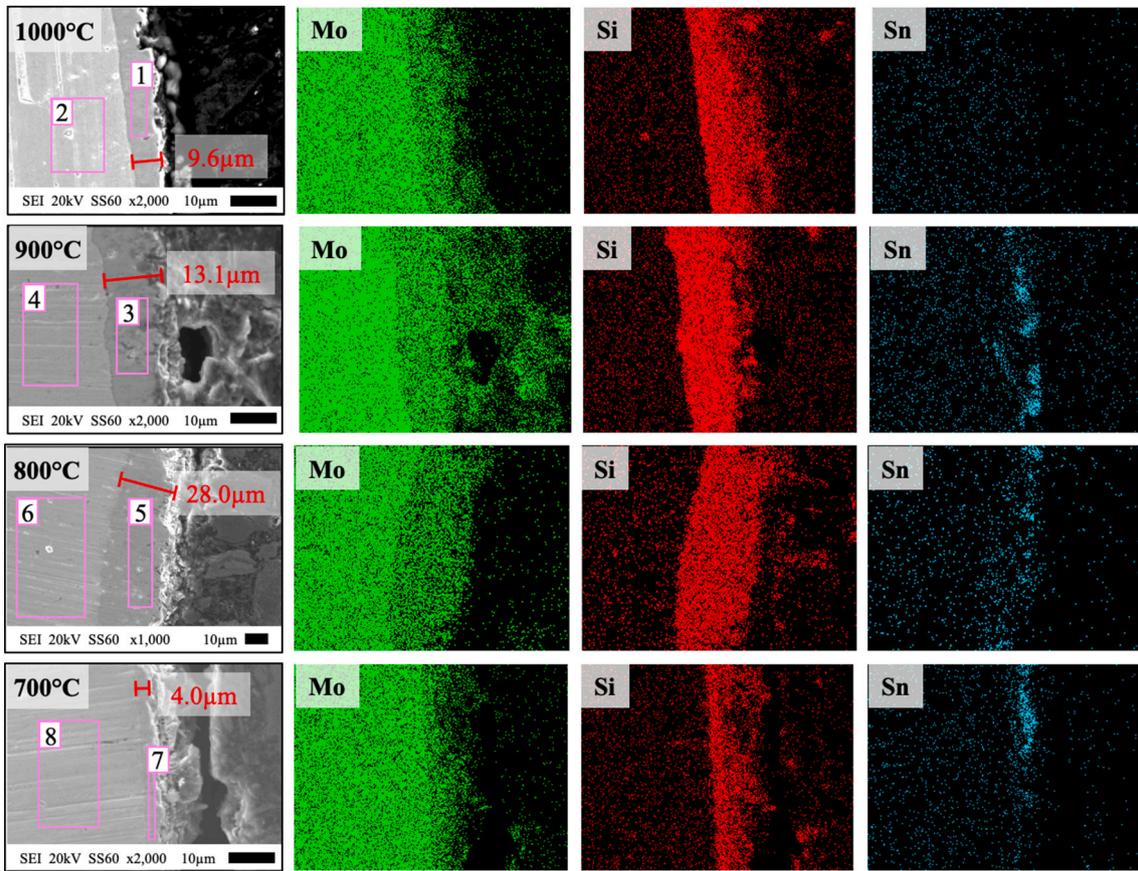
Fig. 3. Cross-section micrographs and EDS mapping of the siliconized samples after hot dipping at 700 °C, 800 °C, 900 °C and 1000 °C for 15 min.

Table 2
Area analysis of the sample cross-section after siliconizing in the molten Sn-Si bath.

Temperature (°C)	Analysis area	Si	Mo	Sn	Phase composition
		(mass%)			
1000	1	34.86	64.55	0.59	MoSi$_2$
	2	0.35	99.45	0.20	Mo-substrate
900	3	33.72	61.60	4.68	MoSi$_2$
	4	0.30	98.90	0.79	Mo-substrate
800	5	33.09	60.49	6.43	MoSi$_2$
	6	0.54	99.33	0.13	Mo-substrate
700	7	30.20	68.26	1.54	MoSi$_2$
	8	0.45	98.98	0.57	Mo-substrate

growth rate was fastest by dipping at 800 °C using the proposed technique. The 45 μm thick MoSi$_2$ layer formed after dipping for 1 h at 800 °C means that the growth of MoSi$_2$ proceeded at 5 times the speed reported for the conventional pack cementation method, which is

carried out at 1300 °C [6]. It is important to note that the simplicity and predictability of the outcome using the proposed technique make it possible to confer the advantages of MoSi$_2$ to large components and complex parts.

3.2. Growth kinetics

To determine the step that limits the growth of the MoSi$_2$ layer using the proposed method, variation in thickness of the formed MoSi$_2$ layer was plotted as a function of time, as shown in Fig. 6. The thickness was an average of six measurements made at different positions in the siliconized sample. The step that governs the growth of the MoSi$_2$ product layer can either be the reaction at the interface or the diffusion through the formed product layer. For a reaction-controlled growth, the thickness of the coating should increase linearly with time according to the following equation:

$$y = kt \tag{1}$$
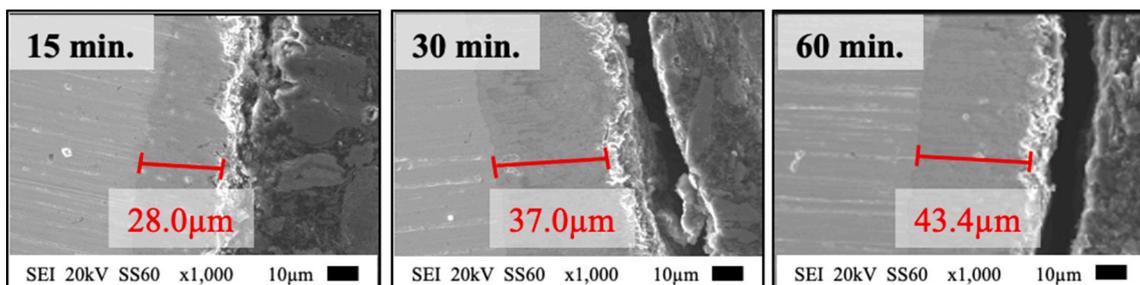
Fig. 4. Cross-section micrographs of the Mo-substrate after hot dipping at 800 °C for 15, 30, and 60 min.
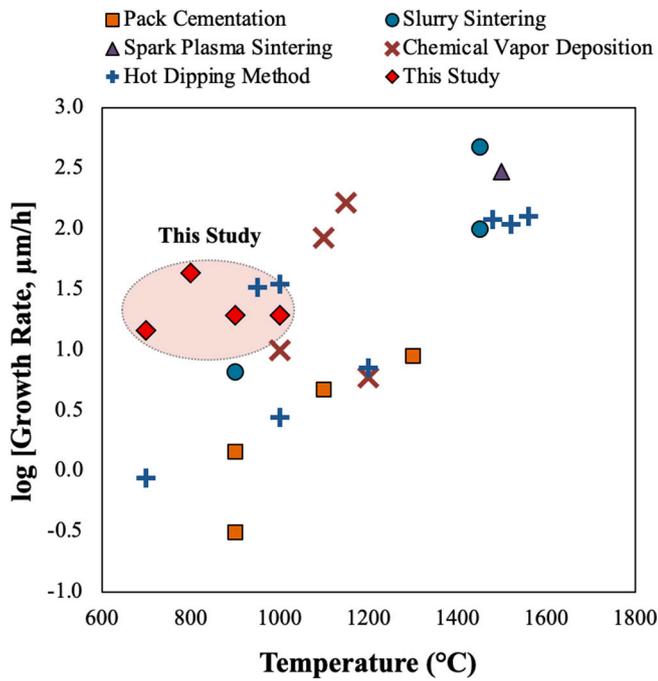
Fig. 5. The MoSi$_2$ growth rates as a function of temperature using different methods: halide-activated pack cementation [6–9], slurry sintering [10–12], spark plasma sintering [13–16], chemical vapor deposition [17–20], the hot dipping method [21–28], and the technique proposed in this study.

where y is the MoSi$_2$ layer thickness at a certain dipping time t for a specific temperature. For a diffusion-controlled growth, the thickness of the coating should increase parabolically with time according to the following equation:

$$y^2 = kt \tag{2}$$

In both above equations, k is the apparent rate constant ($\mu m\ s^{-1}$ or $\mu m^2\ s^{-1}$). Using the measured MoSi$_2$ layer thickness in this study, it was found that by linear regression, R^2 values were closer to unity for the parabolic growth rate, suggesting that siliconization of the Mo-substrate in the Sn-Si melt was a diffusion-controlled process. This suggests that the reaction between silicon and the Mo-substrate occurs much faster

than silicon diffusion through the MoSi$_2$ product layer. In other words, the growth of the MoSi$_2$ layer can be improved by promoting the diffusion of silicon through the formed product layer.

3.3. Variation in the lattice parameters

In the preceding section, it was found that after dipping a Mo-substrate into the Si-saturated tin bath for 15 min at 700 °C to 1000 °C, the formed MoSi$_2$ layer grew fastest at 800 °C, and in this layer, about 6.43 mass% of tin was observed. To explain the rapid growth rate at the dipping temperature of 800 °C, variation in the lattice parameters of the formed MoSi$_2$ layer was investigated.

The x-ray diffraction patterns of the siliconized samples in the range of 38° to 48° with MoSi$_2$ reflection planes (110), (103), and (112) are shown in Fig. 7. The indexed peaks correspond to the characteristic planes of the I4/mmm space group with tetragonal symmetry (ICDD PDF Card No. 041-0612). With increased dipping time, the diffraction peaks of MoSi$_2$ showed a gradual shift towards larger 2θ angles, suggesting a change in the distance between the crystallographic planes. For a tetragonal structure, the lattice constants, a and c, can be determined by the relation:

$$\frac{1}{d_{hkl}^2} = \frac{h^2 + k^2}{a^2} + \frac{l^2}{c^2} \tag{3}$$

where d_{hkl} is the interplanar spacing, and h, k, and l are the Miller indices of the plane. Moreover, the lattice volume, V, can be calculated from the lattice constants using the following equation:

$$V = a^2c \tag{4}$$

The effect of tin concentration measured by SEM-EDS on the diffraction angles, interplanar spacing values, lattice constants, and lattice volume of the formed MoSi$_2$ layers by dipping in a Si-saturated tin bath is summarized in Table 3. It was found that the lattice parameters increased with increasing tin concentration, indicating the displacement of the silicon atoms (1.11 Å) by the larger tin atoms (1.45 Å). Similarly, the variation in lattice volume as a function of tin concentration exhibited the same direct linear relationship with high R^2 values, as shown in Fig. 8. These results suggest that replacement of the silicon atoms with the larger tin atoms led to the expansion of the lattice volume, allowing faster diffusion of silicon through the MoSi$_2$ product layer.

These results reinforce our initial findings that the presence of tin in
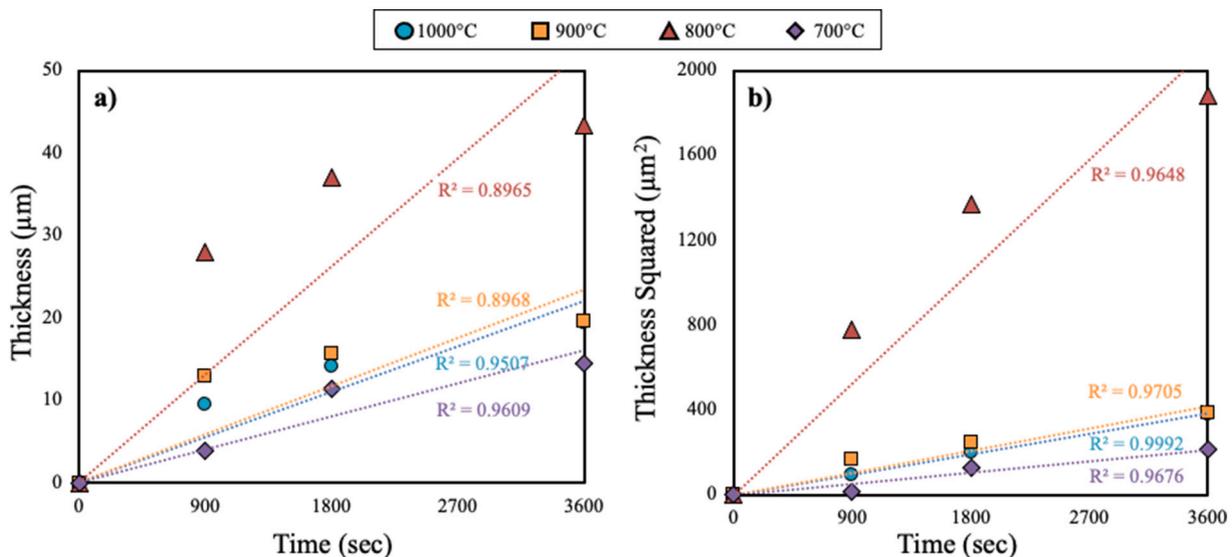
Fig. 6. Plot of MoSi$_2$ layer thickness as a function of time according to (a) reaction-controlled growth mechanism and (b) diffusion-controlled growth mechanism.
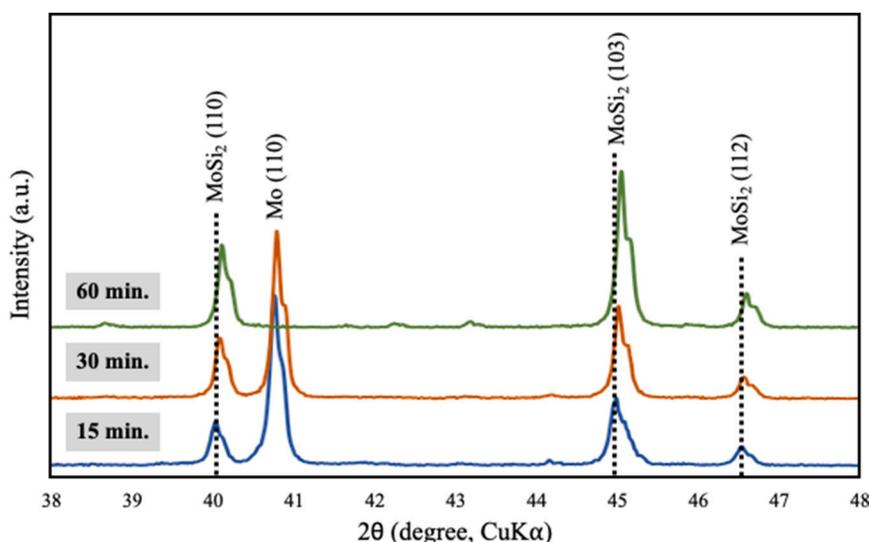
Fig. 7. XRD patterns of the siliconized samples after hot dipping at 800 °C for 15, 30, and 60 min in the range of 38° to 48° showing a gradual shift towards larger 2θ angles with dipping time.

Table 3
Values of the diffraction angles (2θ) of the planes (110) and (103), interplanar spacing (d_{hkl}), lattice constants, and lattice volume of the formed $MoSi_2$ layer as a function of dipping time and tin concentration.

Parameter	Dipping time at 800 °C (min)		
	15	30	60
$2\theta_{(110)}$	40.08	40.10	40.12
$2\theta_{(103)}$	45.00	45.02	45.04
$d_{(110)}$ (Å)	2.248	2.247	2.246
$d_{(103)}$ (Å)	2.013	2.012	2.011
Lattice constant, a (Å)	3.179	3.177	3.176
Lattice constant, c (Å)	7.802	7.799	7.796
Lattice volume, V (Å³)	78.846	78.741	78.635
[Sn] in $MoSi_2$ (mass%)	6.43	4.88	2.22
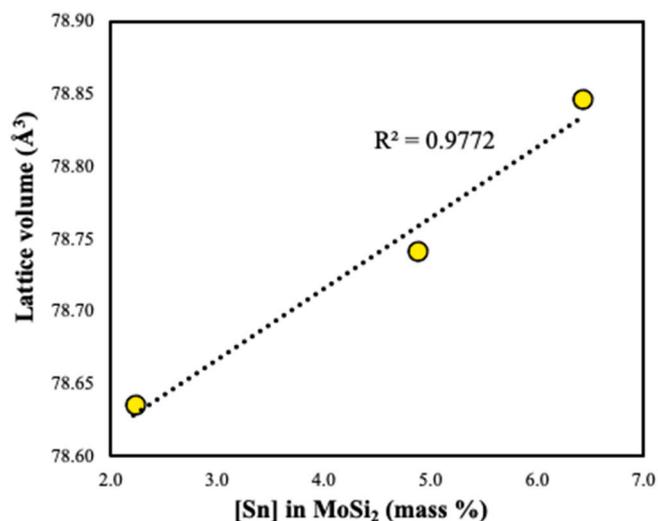
Fig. 8. Tetragonal $MoSi_2$ lattice volume as a function of tin concentration.

the formed $MoSi_2$ layer promoted the faster diffusion of silicon by introducing defects into the structure. Investigation of the growth kinetics in the previous section suggested a diffusion-controlled growth, validating experimental results as to why thicker coatings were observed at the intermediate dipping temperatures of 800 °C. The thickness of the

$MoSi_2$ layer is not only influenced by dipping temperature, but also by the presence of tin in the formed $MoSi_2$ layer. However, due to insufficient thermodynamic and diffusion data on the Sn-$MoSi_2$ system, the mechanism of accelerated tin diffusion at 800 °C remains unknown. This will be determined in a future investigation.

3.4. Oxidation resistance behavior

Although the growth rate of the formed $MoSi_2$ layer was fastest at 800 °C, patches of unmodified molybdenum surfaces were found, as shown by the SEM-EDS image in Fig. 9. EDS mapping indicates that at this temperature, the sample surface was not entirely siliconized by the current method, which is mainly attributed to the increasing density and viscosity of molten tin with decreasing temperature and the poor wettability between molten tin and the Mo-substrate at lower temperatures [31,32]. Since a static hot dipping method was used in the present work, gas packets that form on the surface of the Mo-substrate upon dipping remain in the surface. The density and viscosity of molten tin bath is expected to prevent these gas packets from escaping by floating up to the surface. This means that some surface of the Mo-substrate is not in contact with the bath, and siliconization does not proceed as expected. This problem may be resolved by rotating the sample during the siliconizing process, which is another concern for future investigation.

However, the presence of unmodified molybdenum surfaces makes the sample produced at 800 °C inappropriate for the oxidation resistance test as the bare molybdenum surfaces make it vulnerable to oxidation. Meanwhile, siliconized Mo-substrates prepared at 1000 °C exhibited excellent uniform $MoSi_2$ layer thickness throughout the sample. Therefore, samples dipped at 1000 °C were employed for the oxidation resistance tests.

Sample images of the siliconized Mo-substrates after hot dipping at 1000 °C for 1 h before and after oxidation at 1150 °C for 2 h in air are shown in Fig. 10. As evident from the images, the $MoSi_2$ layer imparted protection of the Mo-substrate from rapid oxidation loss at high temperatures. Sample mass loss of about 4.59 % was observed, which is possibly due to the slight oxidation attack from the cracked portions of the ceramic paste during the oxidation test. The SiO_2 ceramic paste was necessary to protect the uncoated edges of the samples, however, rapid heating and cooling rates caused cracks to form in it, thereby allowing oxygen to penetrate the sample. The slight oxidation attack on the uncoated edges of the sample can be seen as the blue-colored pigmentation in the ceramic paste after the oxidation test. In contrast to the siliconized
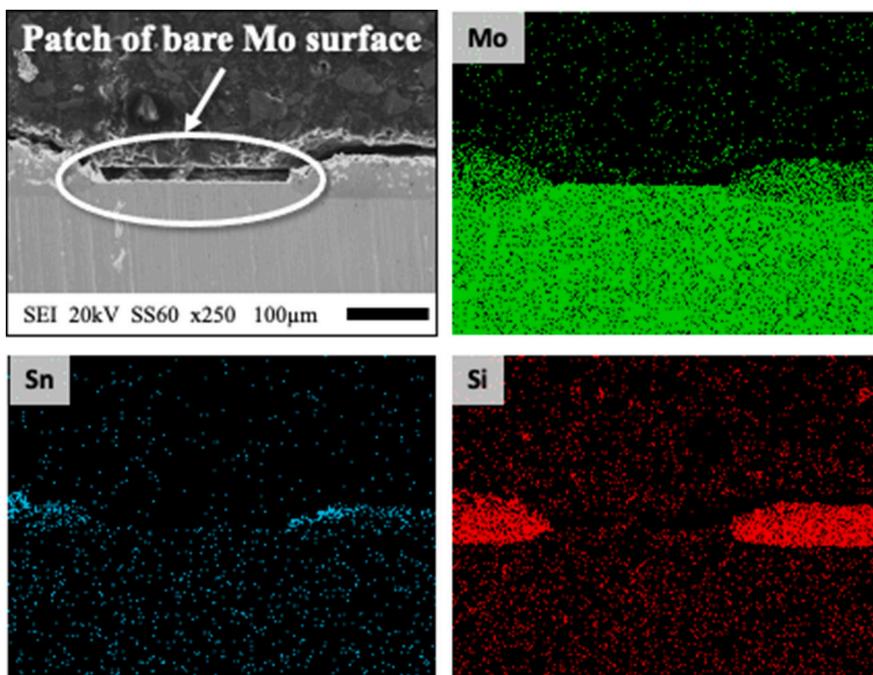
Fig. 9. SEM-EDS micrograph of bare molybdenum surface hot dipped at 800 °C.
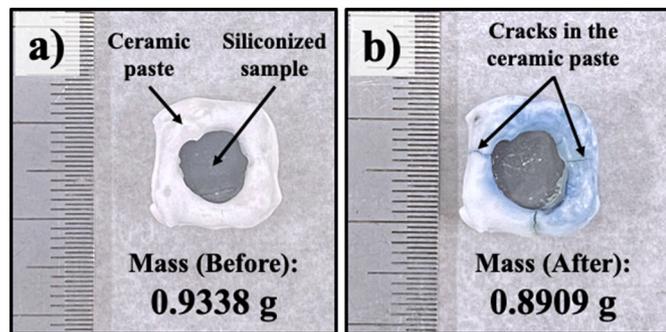
Fig. 10. Siliconized samples a) before and b) after oxidation at 1150 °C for 2 h.

sample, the bare molybdenum sample was completely oxidized and lost in the form of volatile oxides, seen as white fume coming out of the furnace during the oxidation test.

An SEM micrograph, EDS mapping, and a line scan of the sample cross-section after the static oxidation resistance test at 1150 °C for 2 h in air are shown in Fig. 11 and the area analysis results are shown in Table 4. The sample used for the oxidation test had a 20 μm thick MoSi$_2$

Table 4

Area analysis of the MoSi$_2$-coated sample after the isothermal oxidation test at 1150 °C for 2 h in air.

Analysis area	Si	Mo	Sn	Phase composition
	(mass%)			
1	35.41	64.59	–	MoSi$_2$
2	14.30	85.69	0.01	Mo$_5$Si$_3$
3	–	99.78	0.22	Mo-substrate
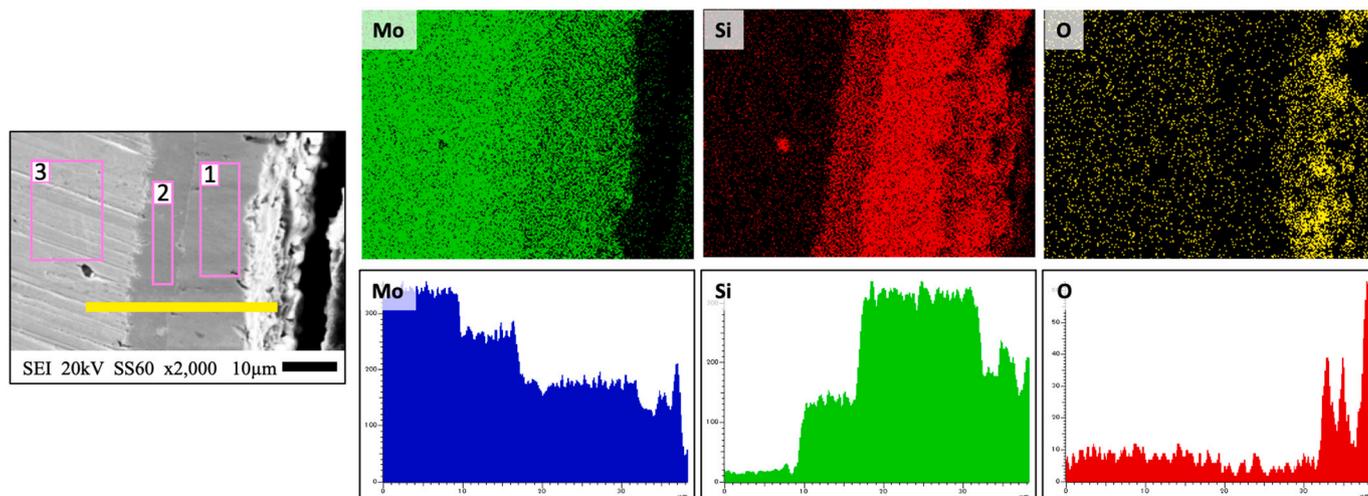
Fig. 11. Cross-section micrographs and EDS analysis of the samples after the static oxidation resistance test at 1150 °C for 2 h in air.

layer formed on the surface of the Mo-substrate after hot dipping in a silicon-saturated tin bath at 1000 °C for 1 h. As evident from the SEM micrograph, the density and uniformity of the $MoSi_2$ layer did not change significantly compared to the as-formed microstructure. After oxidation, the surface of the Mo-substrate consisted three layers – an outer SiO_2 layer followed by the $MoSi_2$ layer and a thin diffusion layer below the primary $MoSi_2$ layer. Area analysis results of the inter-diffusion zone show that Mo:Si atomic ratio is approximately 5:3, indicating that the main phase composition of this layer is Mo_5Si_3. The thickness of the $MoSi_2$ layer and the Mo_5Si_3 inter-diffusion layer were 13.7 μm and 8.6 μm, respectively. EDS mapping and line scan analysis of the sample cross-section shown in Fig. 11 suggest a clear gradient change in molybdenum and silicon concentrations in each of these layers. The formation of other oxidation products, such as Mo_3Si and MoO_3, were not observed in the present work.

It has been reported that the oxidation behavior of $MoSi_2$ strongly depends on temperature and on the partial pressure of oxygen at the reaction interface. The oxidation of $MoSi_2$ coatings can be summarized by the following reactions [33,34]:

$$Si + O_2(g) = SiO_2 \qquad \Delta G^\circ = -858.944 + 0.1754T \qquad (5)$$

$$5/7 MoSi_2 + O_2(g) = 1/7 Mo_5Si_3 + SiO_2 \qquad \Delta G^\circ = -808.260 + 0.1672T \qquad (6)$$

$$3/5 MoSi_2 + O_2(g) = 1/5 Mo_3Si + SiO_2 \qquad \Delta G^\circ$$
$$= -800.038 + 0.1729T \qquad (7)$$

$$2/7 MoSi_2 + O_2(g) = 2/7 MoO_3 + 4/7 SiO_2 \qquad \Delta G^\circ$$
$$= -547.918 + 0.1146T \qquad (8)$$
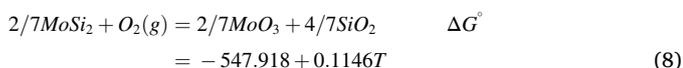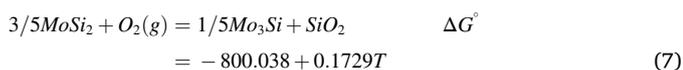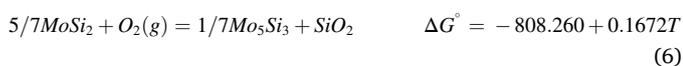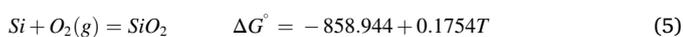
At elevated temperatures, the Gibbs free energy change of the above oxidation reactions is negative. The formation of SiO_2 in Eq. (5) is the most negative, followed by the reaction of $MoSi_2$ with oxygen to form Mo_5Si_3 and SiO_2 in Eq. (6). Meanwhile, the reaction of $MoSi_2$ with oxygen to form MoO_3 and SiO_2 in Eq. (8) is the least negative. These values indicate that the formation of SiO_2 as the oxidation product is most likely to occur at elevated temperatures, followed by Mo_5Si_3, Mo_3Si, and MoO_3.

In this study, the oxidation products were mainly SiO_2 and Mo_5Si_3, which indicates that oxidation reactions in Eqs. (5) and (6) preferentially occurred at 1150 °C after 2 h, thereby preventing the formation of volatile MoO_3. Cross-sectional SEM micrograph of the sample indicates that the $MoSi_2$ layer with Mo_5Si_3 remained dense and smooth at 1150 °C. The SiO_2 outer layer is also known to have self-healing abilities that protect the $MoSi_2$ layer from further oxidation by inhibiting direct contact between oxygen in the atmosphere. The oxidation behavior of the siliconized Mo-substrate using a silicon-saturated molten tin bath in the present work were similar to the results of Zhang et al. that used a pure silicon bath instead [33,35]. In their study, after oxidation at 1200 °C for 2 h, the surface of the coating consisted of SiO_2, $MoSi_2$, and Mo_5Si_3, as it was also observed in the present work. Although oxidation tests at higher temperatures were not conducted, oxidation tests performed by Zhang et al. at 1600 °C indicated the formation of a protective SiO_2 film that effectively filled the micro-cracks on the coating surface.

Therefore, findings in this study suggest that surface modification of the Mo-substrate with $MoSi_2$ using the proposed Si-saturated tin bath effectively protects the Mo-substrate from severe and rapid oxidation at temperatures around 1150 °C and likely higher. Further oxidation tests at higher temperatures and longer holding time with greater sensitivity are required to determine the exact oxidation resistance of the modified surface layer. In addition, appropriate modification to the current method, such as sample rotation, is necessary to ensure uniform thickness of the formed $MoSi_2$ layer at lower temperatures. For the time being, the current work shows the potential of the newly proposed inexpensive and low-temperature Si-saturated tin bath to produce Mo-based components with a modified $MoSi_2$ surface, conferring better oxidation and heat resistance of $MoSi_2$ to those components. In the future, it also has potential use with the Mo-based super alloys expected to replace the current nickel super alloys used in high-temperature oxidizing environments.

4. Conclusions

In this study, the phase composition, growth, and oxidation behavior of a $MoSi_2$ layer formed on a Mo-substrate produced by the hot dipping method using a Si-saturated tin bath was investigated. It was found that a dense $MoSi_2$ layer with a smooth surface can be successfully synthesized using the proposed molten bath at 700 °C, 800 °C, 900 °C, and 1000 °C. The Si-saturated molten tin bath proposed in this study allows $MoSi_2$ to be synthesized more rapidly, and at significantly lower operating temperatures than existing methods. The thickness of the $MoSi_2$ layer grew parabolically with time, indicating that siliconization of the Mo-substrate in the Sn-Si melt is a diffusion-controlled process. The fastest growth rate was at 800 °C and this was due to the faster diffusion of silicon towards the unreacted Mo-substrate because of the expansion of the $MoSi_2$ lattice due to the replacement of the silicon atoms with the larger tin atoms.

The results of the static oxidation resistance test of the siliconized samples at 1150 °C for 2 h in air indicate the formation of an outer SiO_2 layer, a $MoSi_2$ intermediate layer, and a thin Mo_5Si_3 diffusion layer. The SiO_2 outer layer protected the Mo-substrate from further oxidation by inhibiting direct contact between oxygen in the atmosphere. From there, it was found that the siliconization of a Mo-substrate using the proposed Si-saturated tin bath offers protection from rapid oxidation loss at temperatures around 1150 °C.

CRediT authorship contribution statement

Jonah Gamutan: Methodology, Resources, Investigation, Formal analysis, Validation, Writing – original draft, Visualization. **Takahiro Miki:** Conceptualization, Writing – review & editing, Supervision, Project administration, Funding acquisition.

Declaration of competing interest

The authors declare that they have no known competing financial interests or personal relationships that could have appeared to influence the work reported in this paper.

Data availability

Data will be made available on request.

References

[1] A.K. Vasudévan, J.J. Petrovic, A comparative overview of molybdenum disilicide composites, Mat. Sci. Eng. A 155 (1992) 1–17.

[2] D.M. Shah, MoSi2 and other silicides as high temperature structural materials, in: S.D. Antolovich (Ed.), Proc. 7th International Symposium on Superalloys by TMS, 1992, pp. 409–422.

[3] P. Hidnert, W.B. Gero, Thermal expansion of molybdenum, in: Scientific Papers of the Bureau of Standards 19, 1924, pp. 429–440.

[4] S.H. Kamata, D. Kanekon, Y. Lu, N. Sekido, K. Maruyama, G. Eggeler, K. Yoshimi, Ultrahigh-temperature tensile creep of TiC-reinforced mo-si-B-based alloy, Sci. Rep. 8 (2018) 10487.

[5] L. Brewer, R.H. Lamoreaux, The mo-O system, Bull. Alloy Phase Diagr. 1 (1980) 85–89.

[6] J. Sun, Q.G. Fu, L.P. Guo, Y. Liu, C.X. Huo, H.J. Li, Effect of filler on the oxidation protective ability of MoSi2 coating for mo substrate by halide activated pack cementation, Mater. Des. 92 (2016) 602–609.

[7] S. Majumdar, Formation of MoSi2 and Al doped MoSi2 coatings on molybdenum base TZM (Mo-0.5Ti-0.1Zr-0.02C) alloy, Surface & Coatings Technology 206 (2012) 3393–3398.

[8] R. Sakidja, J.S. Park, J. Hamann, J.H. Perepezko, Synthesis of oxidation resistant silicide coatings on Mo-Si-B alloys, Scr. Mater. 53 (2005) 723–728.

[9] K. Ito, T. Murakami, K. Adachi, M. Yamaguchi, Oxidation behavior of mo-9Si-18B alloy pack-cemented in a si-base pack mixture, Intermetallics 11 (2003) 763–772.

[10] W. Li, J. Fan, Y. Fan, L. Xiao, H. Cheng, MoSi2/(Mo, Ti)Si2 dual-phase composite coating for oxidation protection of molybdenum alloy, J. Alloys Compd. 740 (2018) 711–718.

[11] Z. Cai, S. Liu, L. Xiao, Z. Fang, W. Li, B. Zhang, Oxidation behavior and microstructural evolution of a slurry sintered si-mo coating on mo alloy at 1650°C, Surface & Coatings Technology 324 (2017) 182–189.

[12] R. Suzuki, M. Ishikawa, K. Ono, MoSi2 coating on molybdenum using molten salt, J. Alloys Compd. 306 (2000) 285–291.

[13] J. Sun, T. Li, G.P. Zhang, Effect of thermodynamically metastable components on mechanical and oxidation properties of the thermal-sprayed MoSi2 based composite coating, Corros. Sci. 155 (2019) 146–154.

[14] L. Zhu, Y. Zhu, Z. Ren, P. Zhang, J. Qiao, P. Feng, Microstructure, properties and oxidation behavior of MoSi2-MoB-ZrO2 coating for mo substrate using spark plasma sintering, Surf. Coat. Technol. 375 (2019) 773–781.

[15] N. Nomura, T. Suzuki, K. Yoshimi, S. Hanada, Microstructure and oxidation resistance of a plasma sprayed mo-si-B multiphase alloy coating, Intermetallics 11 (2003) 735–742.

[16] G. Reisel, B. Wielafe, S. Steinhäuser, I. Morgenthal, R. Scholl, High temperature oxidation behavior of HVOF-sprayed unreinforced and reinforced molybdenum disilicide powders, Surf. Coat. Technol. 146–147 (2001) 19–26.

[17] J.K. Yoon, J.Y. Byun, H.G. Kim, J.S. Kim, C.L. Choi, Growth kinetics of three mo-silicide layers formed by chemical vapor deposition of Si on mo substrate, Surf. Coat. Technol. 155 (2002) 85–95.

[18] S. Govindarajan, B. Mishra, D.L. Olson, J.J. Moore, J. Disam, Synthesis of molybdenum disilicide on molybdenum substrates, Surf. Coat. Technol. 76–77 (1995) 7–13.

[19] M.J. Rice, K.R. Sarma, Interaction of CVD silicon with molybdenum substrates, J. Electrochem. Soc. 128 (1981) 1368–1373.

[20] A.R. Cox, R. Brown, Protection of molybdenum from oxidation by molybdenum dilicide based coatings, J. Less-Common Metals 6 (1964) 51–69.

[21] Y. Zhang, K. Cui, T. Fu, J. Wang, F. Shen, X. Zhang, L. Yu, Formation of MoSi2 and Si/MoSi2 coatings on TZM (Mo-0.5Ti-0.1Zr-0.02C) alloy by hot dip silicon-plating method, Ceram. Int. 47 (2021) 23053–23065.

[22] Y. Zhang, T. Fu, L. Yu, F. Shen, J. Wang, K. Cui, Improving oxidation resistance of TZM alloy by deposited si-MoSi2 composite coating with high silicon concentration, Ceram. Int. 48 (2022) 20895–20904.

[23] Y. Zhang, L. Yu, T. Fu, J. Wang, F. Shen, K. Cui, H. Wang, Microstructure and oxidation resistance of si-MoSi2 ceramic coating on TZM (Mo-0.5Ti-0.1Zr-0.02C) alloy at 1500°C, Surf. Coat. Technol. 431 (2022), 128037.

[24] Y. Zhang, L. Yu, T. Fu, J. Wang, F. Shen, K. Cui, Microstructure evolution and growth mechanism of si-MoSi2 composite coatings on TZM (Mo-0.5Ti-0.1Zr-0.02C) alloy, J. Alloys Compd. 894 (2022), 162403.

[25] F. Christian, T. Narita, Siliconizing of molybdenum metal in indium-silicon melts, Mater. Trans. JIM 39 (1998) 658–662.

[26] M. Sharifitabar, F. Oukati Sadeq, M. Shafiee Afarani, Synthesis and kinetic study of Mo(Si, Al)2 coatings on the surface of molybdenum through hot dipping into a commercial Al-12wt.%Si alloy melt, Surf. Interfaces 24 (2021), 101044.

[27] M. Nanko, A. Kitahara, T. Ogura, H. Kamata, T. Maruyama, Formation of Mo(Si, Al)2 layer on mo dipped in Al melt saturated with Si and the effects of transition metals added in the melt, Intermetallics 9 (2001) 637–646.

[28] K. Yanagihara, T. Maruyama, K. Nagata, Dip-coating of Mo(Si, Al)2 on mo with an Al-Si melt, Tetsu-to-Hagane 80 (1994) 178–182.

[29] R.W. Olesinski, G.J. Abbaschian, The Si-Sn (silicon-tin) system, Bull. Alloy Phase Diagr. 5 (1984) 273–276.

[30] L. Brewer, R.H. Lamoreaux, The Mo-Sn (molybdenum-tin) system, Bull. Alloy Phase Diagr. 1 (1980) 96–97.

[31] T. Gancarz, W. Gasior, H. Henein, The discharge crucible method for making measurements of the physical properties of melts: an overview, Int. J. Thermophys. 35 (2014) 1725–1748.

[32] J. Saito, Y. Kobayashi, H. Shibutani, Wettability of pure metals with liquid sodium and liquid tin, Mater. Trans. 62 (2021) 1524–1532.

[33] Y. Zhang, Y. Li, C. Bai, Microstructure and oxidation behavior of si-MoSi2 functionally graded coating on mo substrate, Ceram. Int. 43 (2017) 6250–6256.

[34] T. Fu, Y. Zhang, F. Shen, K. Cui, L. Chen, Microstructure and oxidation behavior of si-MoSi2 coating deposited on mo substrate at 600°C and 900°C in static air, Mater. Charact. 192 (2022), 112192.

[35] T. Fu, F. Shen, Y. Zhang, L. Yu, K. Cui, J. Wang, X. Zhang, Oxidation protection of high-temperature coatings on the surface of Mo-based alloys – a review, Coatings 12 (2022) 141.